JOURNAL OF AIRCRAFT
Vol. 46, No. 6, November–December 2009

Engineering Notes

Lateral Stability of High Wing Configurations

William Blake*
U.S. Air Force Research Laboratory, Wright–Patterson Air Force Base, Ohio 45433
and
Carl Gotwald,† Michael Mayor,† and Thomas Cunningham‡
U.S. Air Force Academy, Colorado Springs, Colorado 80848

DOI: 10.2514/1.44911

Nomenclature

AR	=	aspect ratio
b	=	wing span
$C_{l\beta}$	=	variation of rolling moment with sideslip (lateral stability)
d	=	body diameter or diameter of equivalent circular cross section
h	=	body height
w	=	body width
z	=	height of wing above body centerline
κ	=	ratio of airfoil section lift curve slope to 2π, $(C_{l\alpha}/2\pi)$

I. Introduction

THE vertical position of a wing on a body is one of the most significant contributors to lateral stability. Currently used approximations for this effect disagree significantly for configurations with large diameter-to-span ratios. Examples of these types of configurations include swing wings, morphing wings, tube launched systems, etc. This note will show which approximation is the best for this type of configuration.

A body in sideslip experiences crossflow that results in upwash for a high mounted wing in the windward plane and downwash for a low mounted wing. The opposite occurs in the leeward plane. The net effect is a stabilizing rolling moment for high mounted wings and destabilizing moment for low mounted wings. The first theoretical treatment of this effect was given by Multhopp [1]. He used a conformal mapping technique to calculate the rolling moment of a wing mounted on a body of elliptic cross section. After making several simplifications to facilitate the integration, he arrived at the following result

$$C_{l\beta} \approx -2\frac{\mathrm{AR}}{\mathrm{AR}/\kappa+4}\frac{h(h+w)}{b^2}\left[\frac{2z}{h}\sqrt{1-\left(\frac{2z}{h}\right)^2} + \sin^{-1}\left(\frac{2z}{h}\right) - 2\pi\left(\frac{z}{b}\right)\right] \tag{1}$$

for wings mounted on the fuselage and

$$C_{l\beta} \approx -2\pi\frac{\mathrm{AR}}{\mathrm{AR}/\kappa+4}\frac{h(h+w)}{b^2}\left[\frac{1}{2}\left(\frac{|z|}{z}\right) - 2\left(\frac{z}{b}\right)\right] \tag{2}$$

for a wing mounted above or below the fuselage. The Engineering Sciences Data Unit data sheet 73006 [2] uses the Multhopp method [1]. Jacobs [3] and later Levacic [4] graphically integrated the load on a wing induced by the angle-of-attack distribution arising from the potential flow of an infinite cylinder in sideslip. Jacobs [3] presents tables for wings of aspect ratio 5, 7.5, and 10 at three vertical positions on a body with diameter-to-span ratios of 0.1, 0.133, and 0.2. Levacic [4] presents a chart for wings of arbitrary aspect ratio with results for diameter-to-span ratios up to 0.4. The most widely cited approximation is from Campbell and McKinney [5]:

$$C_{l\beta} \approx -1.2\sqrt{\mathrm{AR}}\frac{(h+w)}{b}\frac{z}{b} \tag{3}$$

This is the basis of the method used in the U.S. Air Force Datcom [6] handbook, although the Datcom replaces the body height and width with the diameter of an equivalent circular cross section (Fig. 1), giving

$$C_{l\beta} \approx -2.4\sqrt{\mathrm{AR}}\left(\frac{d}{b}\right)^2\left(\frac{z}{d}\right) \tag{4}$$

II. Results

The existing approximations are in very close agreement for typical configurations ($d/b < 0.3$) and correlate very well with published data [2,6]. However, for configurations with large diameter-to-span ratios, the approximations disagree significantly, even on sign. Before proceeding, the chart developed by Levacic [4] needs to be extended to higher values of (d/b). The proper extrapolation is not obvious based on inspection of the chart. Fortunately, symbolic algebra software now allows an analytic solution to the relevant equation [4,7]:

$$C_{l\beta} \approx \frac{-8\mathrm{AR}}{\mathrm{AR}/\kappa+4}\left(\frac{d}{b}\right)^2\int_{\sqrt{(d/2)^2-z^2}}^{b/2}\frac{y^2 z\sqrt{1-4(y/b)^2}}{(y^2+z^2)^2}\,\mathrm{d}y \tag{5}$$

For a parasol wing or a top or bottom mounted wing, the solution is

$$C_{l\beta} \approx -8\pi\left(\frac{\mathrm{AR}}{\mathrm{AR}/\kappa+4}\right)\left(\frac{d}{b}\right)^2\left[\frac{1+8(z/b)^2}{4\sqrt{1+4(z/b)^2}} - \left(\frac{z}{b}\right)\right] \tag{6}$$

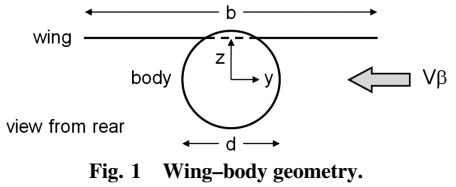

Fig. 1 Wing–body geometry.

Received 13 April 2009; revision received 10 July 2009; accepted for publication 27 July 2009.

*Senior Aerospace Engineer, Air Vehicles Directorate. Associate Fellow AIAA.
†Cadet First Class, Department of Aeronautics. Student Member AIAA.
‡Assistant Professor, Department of Aeronautics. Senior Member AIAA.

For a wing which passes through the body, the result is more cumbersome:

$$C_{l\beta} \approx -8\left(\frac{\mathrm{AR}}{\mathrm{AR}/\kappa + 4}\right)\left(\frac{d}{b}\right)^2\left[\frac{1 + 8(z/b)^2}{4\sqrt{1 + 4(z/b)^2}}\right.$$
$$\times \left\{\pi - 2\tan^{-1}\frac{\sqrt{(d/b)^2 - 4(z/b)^2}\sqrt{1 + 4(z/b)^2}}{2(z/b)\sqrt{1 - (d/b)^2 + 4(z/b)^2}}\right\}$$
$$+ \left(\frac{z}{b}\right)\left\{\frac{\sqrt{(d/b)^2 - 4(z/b)^2}}{(d/b)^2}\sqrt{1 - (d/b)^2 + 4(z/b)^2}\right.$$
$$\left.\left. + 2\sin^{-1}\sqrt{(d/b)^2 - 4(z/b)^2} - \pi\right\}\right] \tag{7}$$

Figure 2 compares the approximations to the data of Goodman and Thomas [8]. They tested an uncambered 60 deg delta wing in low-, mid-, and high-wing positions on three different bodies at low speed. For the low- and high-wing cases, the vertical position was $\frac{1}{3}$ of the body diameter from the centerline. The low-wing results have been multiplied by -1 and are included on the plot. The predictions are essentially identical over the range of body sizes tested. At larger diameter-to-span ratios, they disagree significantly. The Multhopp method [1] appears to be clearly incorrect, with unstable values for the largest body sizes. The error comes from the simplifications made to make the integral tractable. The Campbell and McKinney result [5] grows in proportion to $(d/b)^2$. The analytic solution to Levacic's method [4] shows an increase in lateral stability to a diameter-to-span ratio of about 0.7, then a reduction in stability.

To determine which of the approximations (if any) gives the correct trend for large diameter-to-span ratio, a wind-tunnel test was conducted at the U.S. Air Force Academy Subsonic Wind Tunnel [7]. This is a closed circuit facility with a 3×3 ft test section. The fuselage was 10 in. long with a 2 in. diameter and a 3 in. tangent ogive nose. Five rectangular wings were tested with a root chord of 2 in. and spans corresponding to (d/b) ratios of 0.2, 0.4, 0.6, 0.8, and 1. The fuselage and wings were made of solid aluminum. The wings were untwisted and used a symmetrical NACA 0012 airfoil section. Half of a NACA 0012 airfoil was carved out of the top of the cylindrical body. Holes and screws were covered with wax to ensure smooth flow and limit the amount of flow disruption. A photo of the model in the wind tunnel with the highest span wing is shown in Fig. 3. Tests were run at three different Mach numbers: 0.15, 0.3, and 0.5.

Sample results for the smallest wing and largest wing are shown in Fig. 4. The data are referenced to the area and span of each tested wing. The results are linear in both cases, with correlation coefficients R^2 in excess of 0.99. The smallest wing $(d/b = 1)$ has more than double the lateral stability of the largest wing $(d/b = 0.2)$.

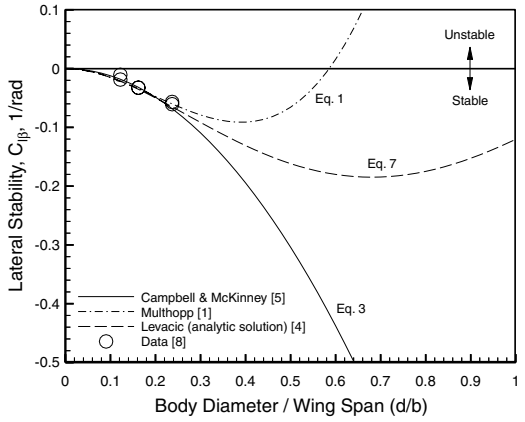

Fig. 2 Effect of diameter-to-span ratio on lateral stability, $(z/d) = \frac{1}{3}$, $\mathrm{AR} = 2.31$, $\kappa = 1$.

Fig. 3 Wing–body model in wind tunnel, $\mathrm{AR} = 5$, $d/b = 0.2$.

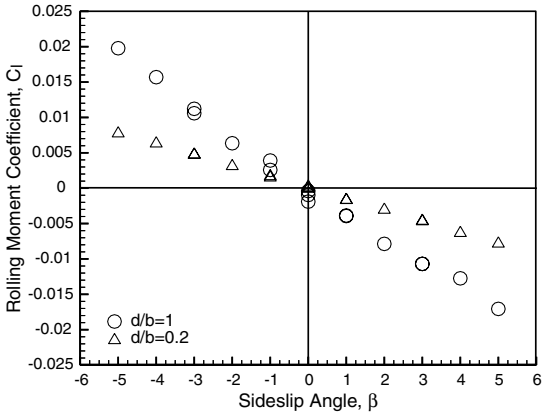

Fig. 4 Effect of sideslip angle on rolling moment, Mach = 0.5.

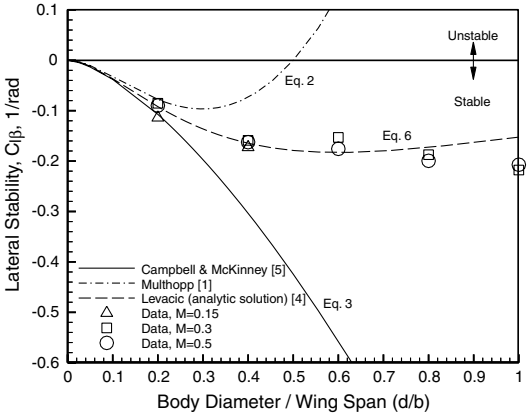

Fig. 5 Effect of diameter-to-span ratio on lateral stability, $(z/d) = 0.5$, $\mathrm{AR} = 1/(d/b)$, $\kappa = 1$.

A complete summary of the results is shown in Fig. 5. For a fixed body size, increases in (d/b) correspond to decreases in wing span. Data points are only shown for the cases where the linear fit was excellent, defined here as $R^2 > 0.95$. All of the Mach 0.3 and 0.5 cases passed this test, whereas only the two largest wings exhibited this degree of correlation at Mach 0.15. For the largest wing $(d/b = 0.2)$, the various theories and data are in close agreement. For the remaining wings, the Levacic method [4] is clearly superior to the other methods. It is within 25% of the test data for all cases; the other methods are off by more than 100% for diameter-to-span ratios in excess of 0.5. For this class of planforms, it predicts the peak value at $d/b = 0.6$. The data show the peak value is reached for the smallest

wing ($d/b = 1$). Whether the values continue to increase beyond this is unknown and is probably of academic interest only due to the very small wing size.

Extensions to the Levacic theory [4] could include expansion to noncircular body cross sections, use of a finite cylinder model, or extension to supersonic flow. Levacic suggests a simple correction of $\frac{1}{2}(1 + w/h)$ for elliptic cross sections. Higher-order computational models can obviously be applied to the problem. The present interest in simple approximations is that these are used by many preliminary design codes, and recent programs have revealed shortcomings in these codes.

III. Conclusions

Existing approximations for the effect of wing height on lateral stability are inadequate for configurations with a large ratio of body diameter to wing span. A closed-form expression for elliptically loaded wings is developed that matches prior approximations for conventional configurations while also giving the correct trends for the large body configurations. For diameter-to-span ratios less than 0.25, all approximations are within 25% of test data. The new approximation maintains this accuracy for diameter-to-span ratios up to 1.0, whereas the prior approximations are off by more than 100% for diameter-to-span ratios in excess of 0.5.

References

[1] Multhopp, H., "Zur Aerodynamik des Flugzeugrumpfe," *Luftfahrtforschung*, Vol 18, Nos. 2–3, March 1941, pp. 52–66; also NACA TM 1036, Dec. 1942 (in English).

[2] Engineering Sciences Data Unit, "Effects of Isolated Body and Wing-Body Interference on Rolling Moment Due to Sideslip," Data Sheet 73006, Amendment C, London, March 1999.

[3] Jacobs, W., "Berechnung des Schiebe-Rollmomentes fur Flugel-Rumpfanordnungen," *Jahrbuch der Deutschen Luftfahrtforschung*, 1941, pp. 165–171.

[4] Levacic, I., "Rolling Moment Due to Sideslip, Part III: The Effect of Wing Body Arrangement," Royal Aircraft Establishment, Rept. Aero.2139, 1946.

[5] Campbell, J.P., and McKinney, M.O., "Summary of Methods for Calculating Dynamic Lateral Stability and Response and for Estimating Lateral Stability Derivatives," NACA TR 1098, 1952.

[6] Hoak, D. E., Finck, R. D., Ellison, D. E., and Malthan, L. V., "USAF Stability and Control Datcom," U.S. Air Force Wright Aeronautical Lab. TR 83-3048, Wright–Patterson AFB, OH, Oct. 1960 (revised 1978).

[7] Blake, W. B., Gotwald, C., Mayor, M., and Cunningham, T., "Lateral Stability of High Wing Configurations," *AIAA Atmospheric Flight Mechanics Conference*, AIAA Paper 2009-6044, Aug. 2009.

[8] Goodman, A., and Thomas, D. F., Jr., "Effects of Wing Position and Fuselage Size on the Low-Speed Static and Rolling Stability Characteristics of a Delta-Wing Model," NACA TR 1224, 1955.